



Deposited via The University of Sheffield.

White Rose Research Online URL for this paper:

<https://eprints.whiterose.ac.uk/id/eprint/158532/>

Version: Accepted Version

Article:

Beamish, S., Li, X., Brunskill, H. et al. (2020) Circumferential film thickness measurement in journal bearings via the ultrasonic technique. *Tribology International*, 148. 106295. ISSN: 0301-679X

<https://doi.org/10.1016/j.triboint.2020.106295>

Article available under the terms of the CC-BY-NC-ND licence (<https://creativecommons.org/licenses/by-nc-nd/4.0/>).

Reuse

This article is distributed under the terms of the Creative Commons Attribution-NonCommercial-NoDerivs (CC BY-NC-ND) licence. This licence only allows you to download this work and share it with others as long as you credit the authors, but you can't change the article in any way or use it commercially. More information and the full terms of the licence here: <https://creativecommons.org/licenses/>

Takedown

If you consider content in White Rose Research Online to be in breach of UK law, please notify us by emailing eprints@whiterose.ac.uk including the URL of the record and the reason for the withdrawal request.

Circumferential Film Thickness Measurement in Journal Bearings via the Ultrasonic Technique

S. Beamish*, X. Li, H. Brunskill, A. Hunter, R. Dwyer-Joyce
Department of Mechanical Engineering, University of Sheffield, Sheffield, UK
*sbeamish1@sheffield.ac.uk

Abstract

A key parameter in hydrodynamic journal bearing performance is lubricant layer thickness around the circumference of the shaft-bearing interface. In the present work, the ultrasonic amplitude, phase change and resonant dip techniques are applied to obtain circumferential film thickness profiles in a bespoke journal bearing test platform under a range of shaft-aligned, shaft-misaligned and shut-down operating conditions. Film thickness results are compared against the Raimondi-Boyd theoretical prediction model and eddy current sensor measurements. By using an on-line referencing technique, the amplitude and phase change models demonstrated high accuracy for thin films and the resonant dip technique enabled film measurements within the bearing thick film region. Thus, applying the three methods simultaneously allowed analysis of lubricant films around the bearing circumference.

Keywords

oil film thickness measurement, ultrasound, journal bearing, phase change, circumferential, misalignment, shut-down.

I. INTRODUCTION

The efficiency of a hydrodynamic journal bearing is highly dependent on lubricant film thickness at its interface. Too thin and the surfaces will contact, leading to excessive wear and friction. Conversely, if the film is too thick, additional energy is needed to shear the lubricant unnecessarily, leading to increased friction due to viscous losses. Thus, there is a sweet-spot in which lubricant film thickness is just right, with friction and wear at its lowest.

Current film thickness prediction techniques are satisfactory for many bearing design applications. However, for high precision or highly loaded systems a more direct measurement approach is often required [1]. For example, the use of environmentally acceptable lubricants (EALs) in marine stern tube bearings has proven challenging, leading to unprecedented wear and failure rates. It has been proposed that this may be due to shear thinning under extreme conditions [2, 3], however further analysis is required to support these claims, including the simulation of such conditions in a real system.

Due to the journal bearing's enclosed geometry and the minute thickness of the oil film, typically in the order of 1's to 10's microns, conventional techniques often struggle to provide effective measurements. Eddy current sensing for example is a popular method, allowing measurements over a wide range of film thicknesses. However, the probes must be positioned within the contact for a direct measurement, which interferes with the fluid film [4]. Mounting sensors away from the contact negates these effects, although factors such as deformation in the components introduces uncertainties. Therefore, the technique is either invasive if probes are positioned within the contact or loses accuracy if positioned outside the contact. Additionally, eddy current sensors are restricted to conductive materials, require precise calibration and are susceptible to noise from external sources [4, 5].

Optical interferometry is a technique which observes the phase difference between light beams reflected from each boundary; enabling film thickness measurements to sub-micron precision. However, the method requires at least one of the surfaces to be transparent, thereby limiting the number of suitable materials [6].

A promising alternative is the ultrasonic method. Ultrasonic sensors are non-invasive in nature as they are mounted away from the area of interest, either embedded inside the shaft or on the bearing shell outer surface. Therefore, a direct measurement at the contact can be obtained without the hardware influencing the system. Furthermore, the technique is effective for a wide range of engineering materials such as steels and polymers [7].

As the ultrasonic technique matures, it is being applied to ever more complex scenarios. Previous studies often focus on film thickness measurements at a single point [8], however effects such as cavitation and bearing deformation require a more complete circumferential film thickness profile of the bearing [9]. Additionally, more anomalous operating conditions are of interest, such as the behaviour of misaligned shaft-bearing interfaces or how an oil film develops during shut-down conditions, particularly as start-stop technology in automotive applications becomes ever more popular [10].

In this investigation, three ultrasonic methods are applied simultaneously to a bespoke journal bearing test platform operating under a series of test conditions. This bespoke journal bearing test rig has been instrumented with ultrasonic transducers embedded within the shaft, so that circumferential film thickness profiles may be obtained, allowing the study of common journal bearing phenomena such as cavitation and bearing shell deformation.

II. ULTRASONIC MEASUREMENT TECHNIQUES

The ultrasonic method has been previously demonstrated as a robust, high accuracy technique in the measurement of thin lubricant films, with theoretical principles well understood [11, 12, 13]. The following is a summary of how acoustic response may be linked to lubricant film thickness.

A. Amplitude and Phase Change Techniques

If the wavelength of an ultrasonic signal is large compared to the thickness of a lubricant film and if it is normally incident to the interface, then the interface may be treated as a unique reflector [11]. As such, the proportion of the wave reflected, known as the reflection coefficient, R , is dominated by the interfacial stiffness of the boundary. This may be expressed by:

$$|R| = \frac{A_R}{A_I} = \sqrt{\frac{(\omega z_1 z_2)^2 + K^2(z_2 - z_1)^2}{(\omega z_1 z_2)^2 + K^2(z_2 + z_1)^2}} \quad (1)$$

Where A_R denotes the reflected signal amplitude, A_I is the incident signal amplitude, ω is the angular frequency of the ultrasonic wave, z_1 and z_2 are the acoustic impedance of the materials either side of the lubricant film and K is the stiffness per unit area of the lubricant film. Acoustic impedance is a measure of the resistance to acoustic flow within a material and is a function of the material's density and acoustic velocity [14].

The stiffness of this boundary, may be related to the thickness and acoustic properties of the film by:

$$K = \frac{B}{h} = \frac{\rho c^2}{h} \quad (2)$$

Where B is bulk modulus, ρ is lubricant density, h is lubricant film thickness and c is acoustic velocity of the lubricant.

Combining Equations 1 and 2, a relationship between reflected signal amplitude and film thickness, may be formulated:

$$h = \frac{\rho c^2}{\omega z_1 z_2} \sqrt{\left(\frac{R^2(z_2 + z_1)^2 - (z_2 - z_1)^2}{1 - R^2} \right)} \quad (3)$$

The phase of the reflected signal is also related to the stiffness of the interface, this can be expressed mathematically as:

$$\phi_R = \arctan\left(\frac{2\omega z_1 z_2^2 / K}{(z_2 - z_1) + \omega^2(z_1 z_2 / K)^2}\right) \quad (4)$$

Combining Equations 2 and 4, a similar relationship between thickness and the change in phase of the signal may be formulated:

$$h = \frac{\rho c^2 (\tan \phi_R) (z_2^2 - z_1^2)}{\omega z_1 z_2^2 \pm \sqrt{(\omega z_1 z_2^2)^2 - (\tan \phi_R)^2 (z_2 - z_1^2) (\omega z_1 z_2)^2}} \quad (5)$$

Therefore, if the acoustic properties of the system are known, the reflected signal may be used to determine the thickness of an oil film, either by observing its proportional change in amplitude or its change in phase. The relationship between film thickness, amplitude and phase for a range of centre frequencies is shown in Figure 1. In this example the interface materials are steel and leaded bronze separated by a mineral oil. This configuration is used in the present study and is commonly found in bearing systems.

Figure 1 highlights that there is a practical limit to the measurement range of each technique. As film thickness increases, the system is no longer stiffness dominated and each model tends to a constant value, $R \rightarrow 1$ for Equation 3 and $\phi \rightarrow 0$ for Equation 5. Thus, the film thickness measurement becomes indistinguishable from background noise. This limit is dictated by a number of factors including signal quality and can be increased by averaging multiple captures. A maximum reflection coefficient of 0.99 and minimum phase change of 0.025 radians are applied in this example.

Comparing the bounds formed by each practical measurement region, it can be seen that the phase change technique is capable of measuring thicker films compared to the amplitude technique. For example, in Figure 1 a centre frequency of 20MHz allows a maximum film thickness measurement of 4 μm via the amplitude technique and 20 μm via the phase change technique under the same conditions.

It is therefore imperative to select transducers with an appropriate centre frequency so that the full film thickness range of interest may be measured. Incorporating multiple sensors of varying frequencies may extend this range further if necessary, although this increases the complexity of the measurement system.

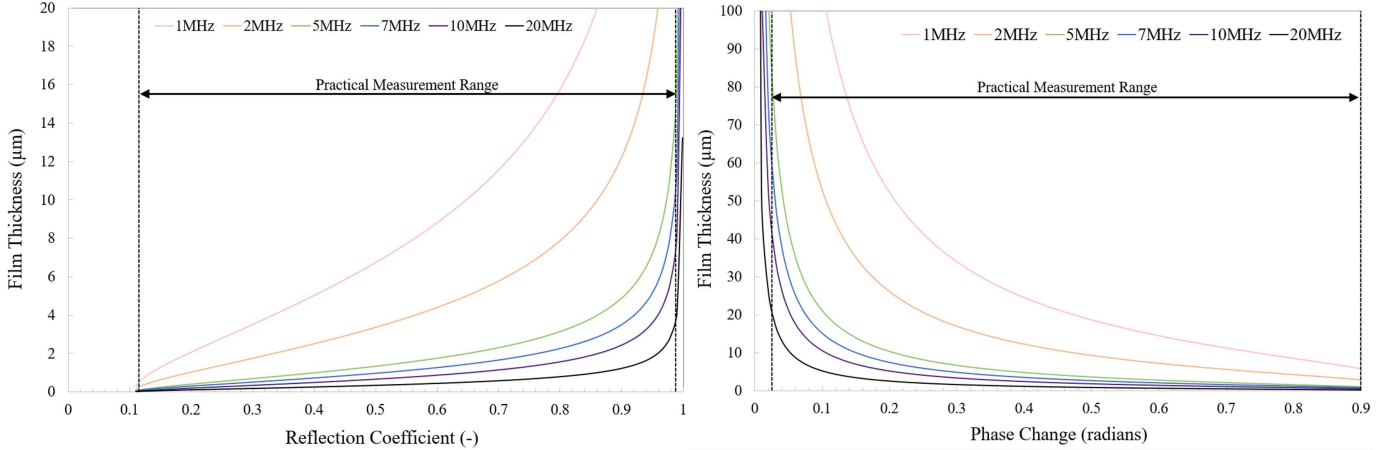


Fig. 1: The relationship between film thickness and reflection coefficient (left), film thickness and phase (right) for an oil lubricated steel-led bearing bronze interface, with practical measurement regions defined.

B. Resonant Dip Technique

The resonant dip ultrasonic technique may be applied to measure thick films outside the measurement range of both the amplitude and phase change techniques [15]. When lubricant thickness matches the resonant frequency of the transducer, the lubricant layer will resonate. This manifests as an amplitude dip in the frequency domain. By tracking the frequency at which this dip occurs, film thickness may be calculated via the following equation.

$$f_m = \frac{cm}{2h} \quad (6)$$

Where f_m is the dip frequency, and m is the resonance mode.

A theoretical example is shown in Figure 2, with each fundamental frequency dip feature annotated with a corresponding film thickness, determined by Equation 6. In the example acoustic velocity is 1352 m/s . This corresponds to the acoustic velocity of the mineral oil used in the current study at 65°C. Additional dips are present at higher resonance modes. These can also be used in film thickness measurements, however as the higher order dips are less pronounced it can be difficult to distinguish these features from background noise.

III. JOURNAL BEARING TEST PLATFORM

A bespoke journal bearing test platform has been designed and commissioned with the capabilities of circumferential film thickness measurements via ultrasonic transducers embedded in the shaft. A schematic and photograph of the bearing platform are shown in Figures 4 and 5 respectively.

In this design, two spherical rolling element bearings support a rotating shaft in a fixed axial position. A journal bearing located between these support bearings is free to articulate in multiple degrees of freedom via a flexible linkage; such that when load is applied via a hydraulic actuator the floating bearing assembly may find its natural position. This ensures the shaft and bearing are aligned. The journal bearing assembly is flooded with lubricant, which is continuously circulating. Flooding the assembly ensures starvation will not occur during testing. Lubricant is stored in a heated circulation bath, which allows accurate lubricant inlet temperature control. A schematic of the journal bearing, including oil inlet position at 27°, is shown in Figure 3, with ϕ denoting attitude angle.

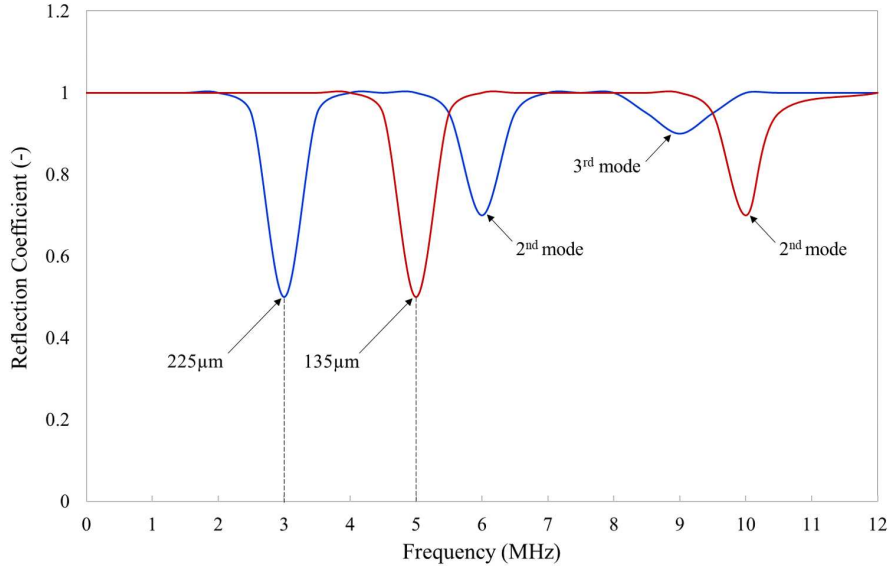


Fig. 2: Example of resonant dips for two theoretical cases, with corresponding film thickness shown for the fundamental dip frequencies. Higher order resonance modes are also identified.

TABLE I: Test platform operating parameters.

Parameter	Value
Bearing radial clearance, C	$50 \mu\text{m}$ ($+0 - 5 \mu\text{m}$)
Bearing internal diameter, D	112.08 mm
Bearing length, L	50.55 mm
Load range, W	2-20 kN
Rotation speed, N	100-800 rpm
Ultrasonic acquisition rate	80 kHz

Additional measurement hardware is also installed on the test platform. K-type thermocouples monitor temperature within the bearing assembly, oil bath and oil inlet. A load cell monitors applied load and an encoder records rotation angle. Four eddy current gap sensors are located on the outside of the bearing assembly to enable indirect film thickness measurements. The locations of these gap sensors are shown in Figure 6.

A flow diagram showing the connections between each measurement hardware item is displayed in Figure 7. The test platform specifications and operating parameters used in the present investigation are shown in Table I.

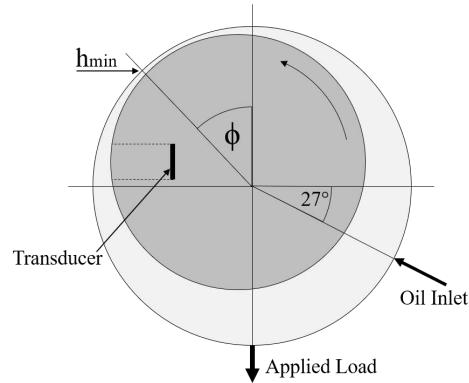


Fig. 3: Schematic of bearing geometry including position of oil inlet, with ϕ denoting attitude angle.

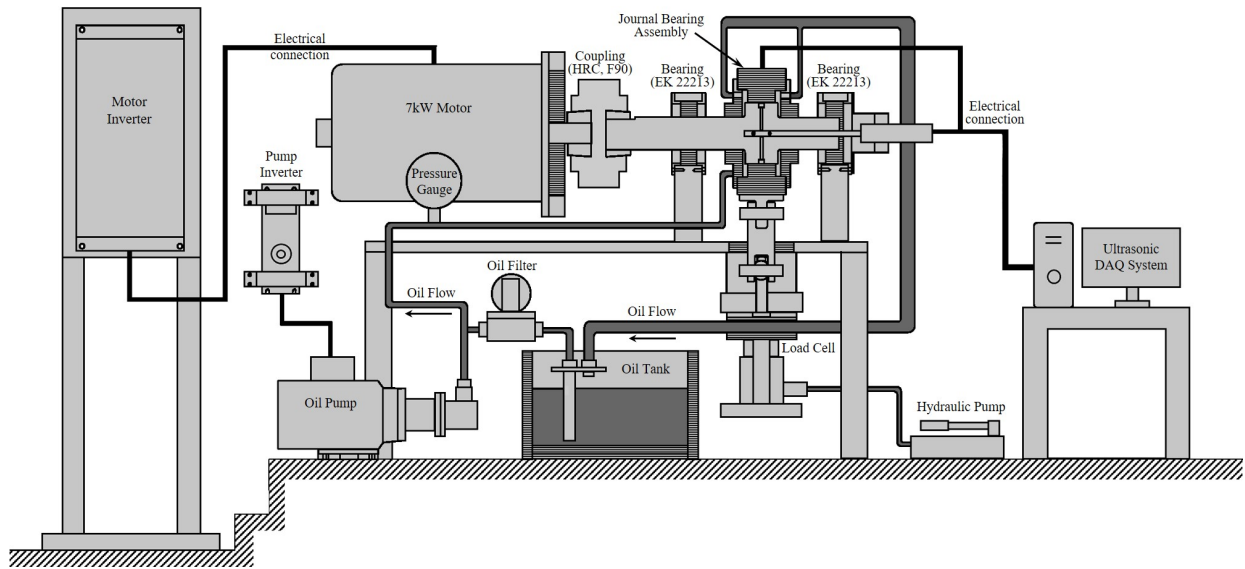


Fig. 4: Schematic of journal bearing test platform.

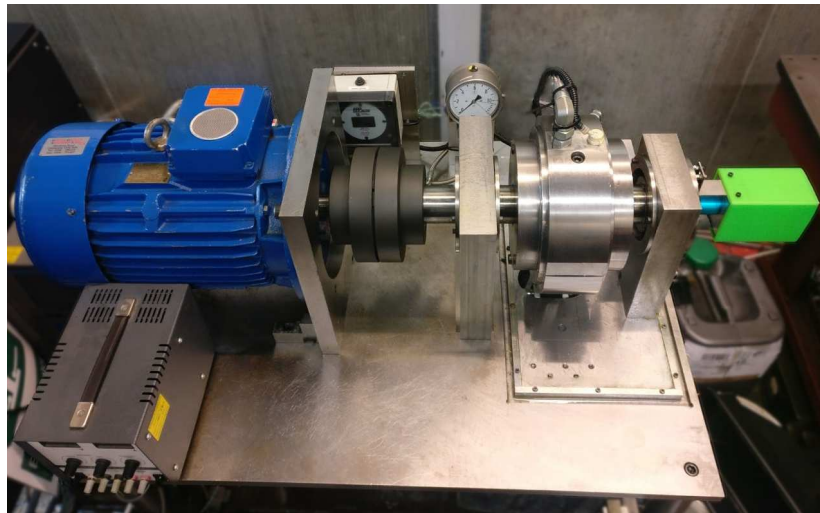


Fig. 5: Photograph of journal bearing test platform.

IV. HOLLOW SHAFT INSTRUMENTATION

This test platform includes six longitudinal ultrasonic transducers embedded within the shaft, the layout of which is displayed in Figure 8. Each transducer connects to the data acquisition hardware via a multi-channel slip ring. Piezoceramic elements are permanently bonded onto a steel pin using epoxy-phenolic strain gauge adhesive. The pin is potted with epoxy resin for protection against mechanical damage and oil ingress. A photograph and schematic of the pin design is shown in Figure 9.

As shown in Figure 10, these pins are then inserted into the shaft and bonded in place. The running surface is reground after pin installation to ensure the transducer assembly has no influence on the shaft-bearing interface during operation. Both the pin and shaft materials are EN24 steel. This ensures the pin does not experience compressive stresses during elevated temperatures. The use of dissimilar materials would lead to the acoustoelastic effect, in which external stresses would cause a change in the wave velocity of the pin [16]. This would result in a time-of-flight change of the reflected signal, thus affecting the film thickness measurement.

Table II shows the material properties of the primary components and lubricant used in this investigation. The lubricant used in the present study is a high-performance marine diesel engine mineral oil.

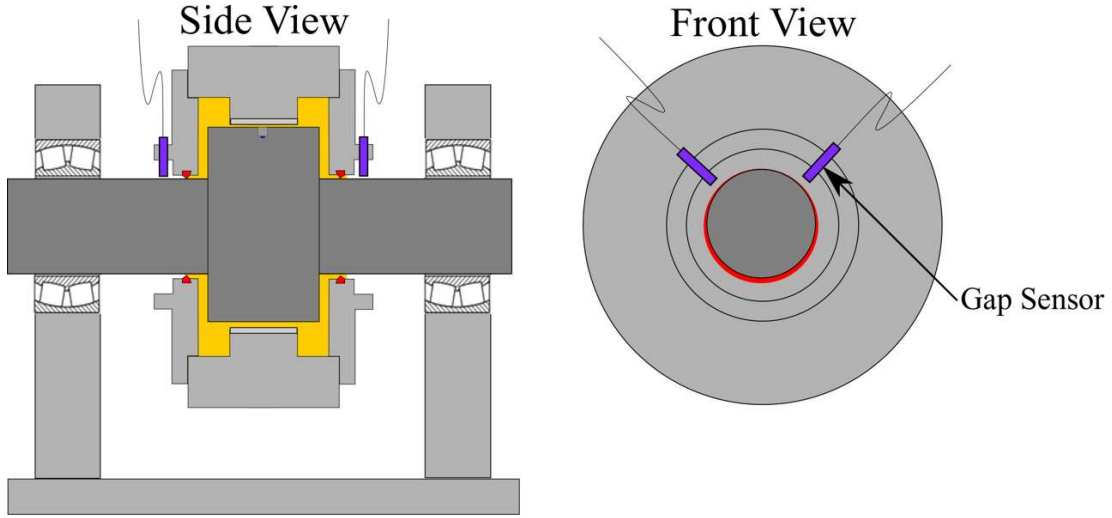


Fig. 6: Partial schematic of journal bearing test platform with gap sensor locations indicated.

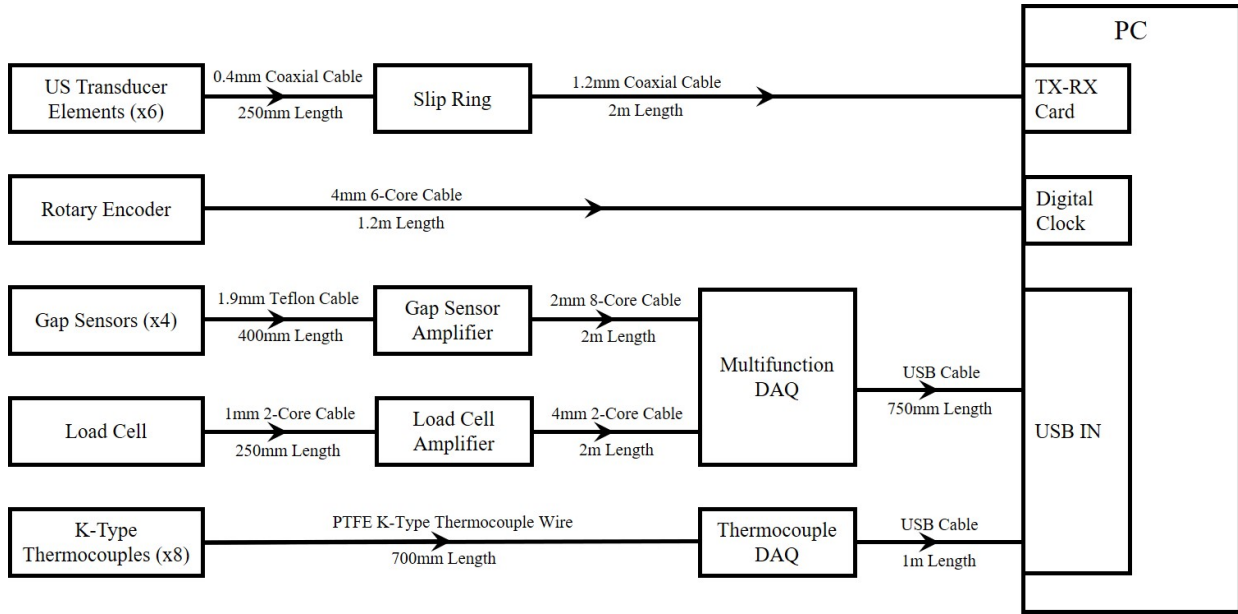


Fig. 7: Measurement hardware flow diagram.

TABLE II: Material properties.

Material Property	Value
Acoustic impedance of bearing, z_2	37.1 MRayl
Acoustic impedance of shaft, z_1	46 MRayl
Oil density, ρ	$888/(1 + 0.0007(T - 20)) \text{ kgm}^{-3}$
Oil acoustic velocity, c	$(0.0039T^2 - 3.39T + 1555.2) \text{ ms}^{-1}$
Oil kinematic viscosity @ 40°C	104 cP
Oil kinematic viscosity @ 100°C	11.6 cP
Ultrasonic wave centre frequency, f	7 MHz

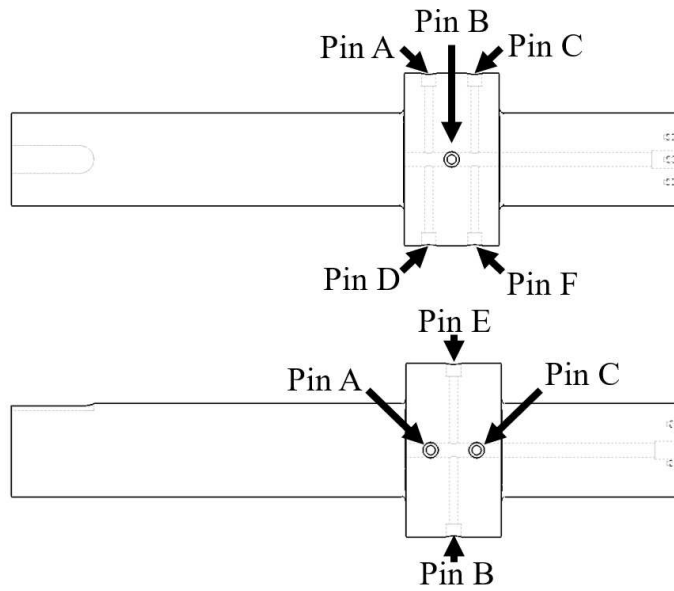


Fig. 8: Schematic of instrumented shaft showing pin layout.

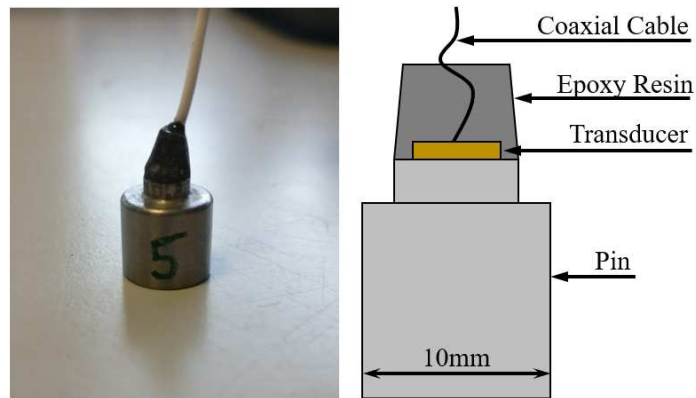


Fig. 9: Photograph (left) and schematic (right) of instrumented pin.

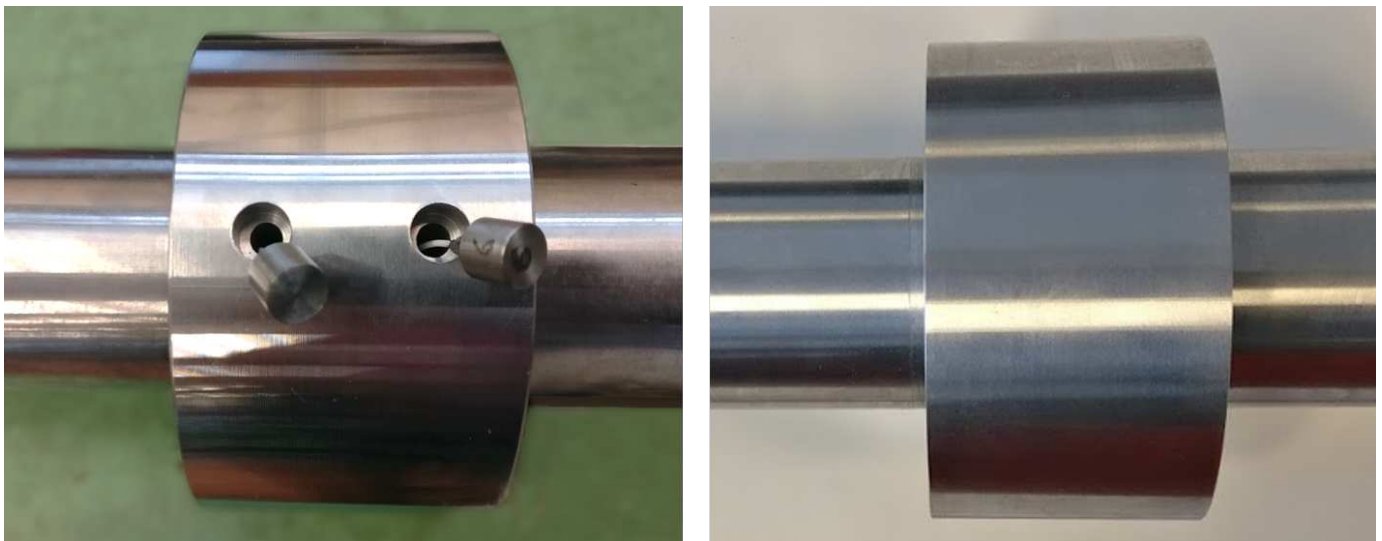


Fig. 10: Photograph of (left) shaft pin installation, (right) shaft after grinding.

V. FILM THICKNESS ACQUISITION METHODOLOGY

Reflection coefficient can be found for each measurement by comparing the proportional amplitude of the measurement signal against a reference signal at a particular frequency. The selected frequency is known as the index frequency. 7 MHz has been used in this investigation as it is close to peak amplitude, thus providing an optimum signal to noise ratio. Similarly, the phase change can be calculated by subtracting the reference phase from the measurement phase at the index frequency. An example time-domain signal and corresponding frequency-domain signals calculated via a fast Fourier transform is shown in Figure 11.

Mapping these values against encoder data, the change in reflection coefficient and phase may be found per degree across the whole shaft rotation. Note that for clarity in the following results top-dead-centre does not correspond to 0° rotation angle and has been annotated where appropriate. Figure 12 shows the change in reflection coefficient and phase as the shaft rotates for a typical test case (100 rpm, 10 kN). Three distinct regions may be observed, these are the thin film, 'infinite' film and resonance regions. These regions are found in all test cases performed in the present study.

Within the thin film region, between 0° and 145° in Figure 12, there is a steady decrease followed by a steady increase in reflection coefficient as the surfaces converge and diverge. Similarly, phase difference steadily increases then decreases.

In the 'infinite' film region, between 145° and 235°, the oil film is thick enough that it is out of range for both the amplitude and phase techniques. Therefore, the reflection coefficient tends to unity and phase change tends to zero. It will be shown later in this section that the 'infinite' film region is a useful feature in obtaining a reference for ultrasonic film thickness measurement.

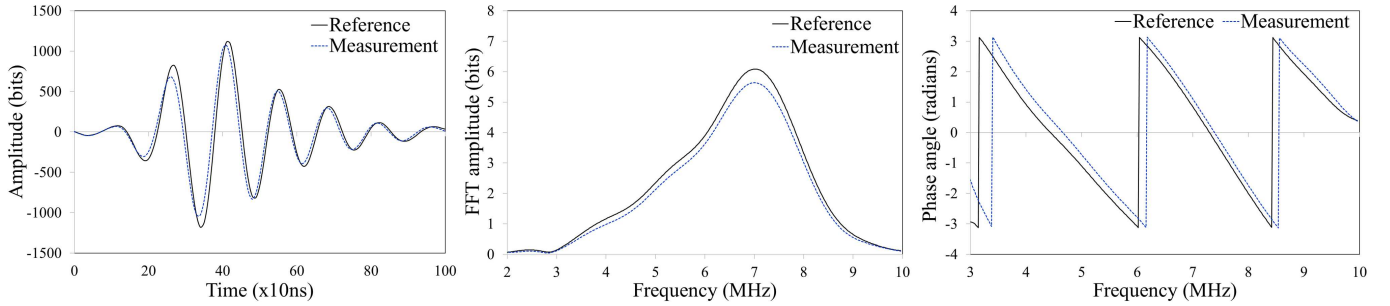


Fig. 11: Example time domain signal (left) and corresponding calculated FFT amplitude (centre) and phase (right) plots.

Within the resonance region, between 235° and 360°, the thickness of the film matches the resonant frequency of the transducer. This causes the lubricant layer to resonate, leading to dips in reflected wave energy at certain frequencies. This manifests in Figure 12 as sharp variations in both phase and reflection coefficient.

By applying Equations 3 and 5, the film thickness profile across the circumference may be calculated via the amplitude and phase change models respectively.

Previous work typically used a static air reference taken prior to or after testing [4, 17]. This is a simple technique which requires only a single comparative measurement. However, the method can lead to significant inaccuracies. Firstly, as the test platform continues to operate, frictional heating causes the temperature of the instrumented shaft, and therefore the piezo-electric element, to increase. These temperature variations affect the energy output from the transducer. Additionally, the bond line between the element and shaft pin are subject to temperature variations [11]. These effects may be mistaken as an exaggerated change in reflection coefficient or phase change if compared against a static air reference.

In the present study, an alternative referencing technique is applied. The 'infinite' film region is used as a near-simultaneous, on-line reference for each test case. This provides a more accurate result as the time delay between reference and measurement is too small for frictional heating to significantly increase piezo-electric element temperature. Also, this technique offers some practical benefits as the test platform does not require disassembly for a new reference to be taken.

To investigate thick films, the resonant dip technique may be applied. By observing reflection coefficient across the full frequency range, a sharp reduction in reflected wave energy will occur at a particular location. This corresponds to the resonant frequency of the lubricant layer and thus can be used to determine film thickness via Equation 6. An example

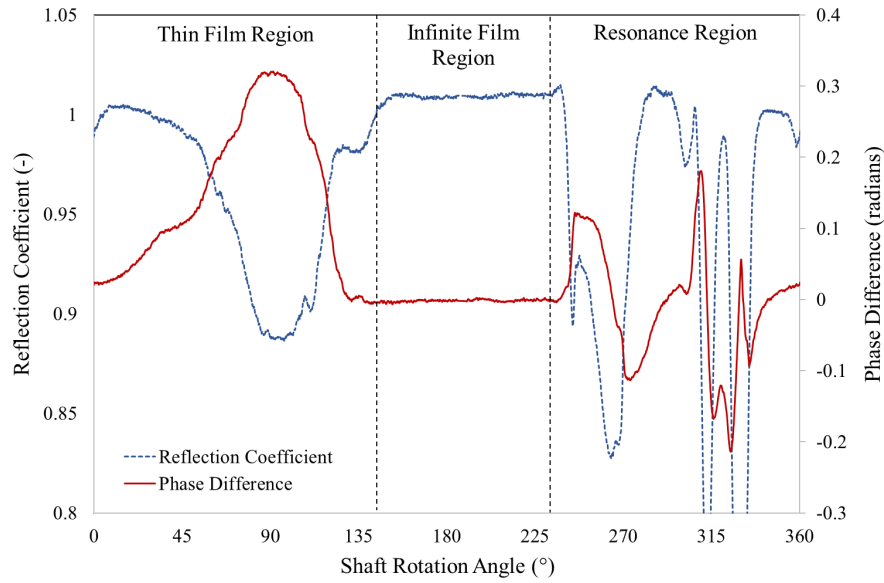


Fig. 12: Reflection coefficient and phase change for a typical full 360° shaft rotation, 100 rpm, 10 kN. Thin film, 'infinite' film and resonance regions are also indicated.

resonant dip acquired in the present study is shown in Figure 13. A usable bandwidth of -12 dB of peak amplitude has been applied as reflection coefficient measurements are affected by noise to a greater extent with decreasing FFT amplitude.

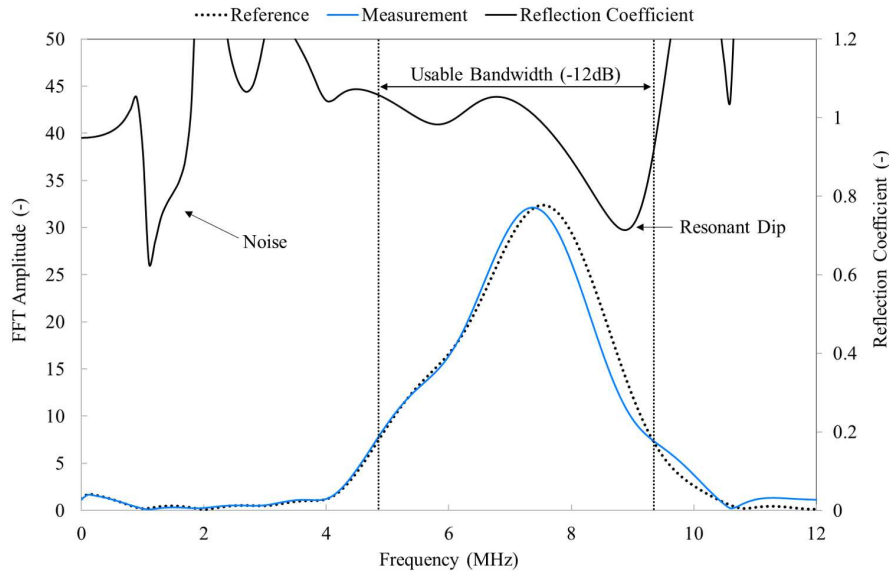


Fig. 13: Signal amplitude in the frequency domain for an example test case and reference. The corresponding reflection coefficient is shown, with a resonant dip indicated.

VI. RESULTS

A. Aligned Bearing Testing

To understand operation of the journal bearing system under normal operating conditions a series of tests under constant rotation speeds and applied loads was performed. The current work reports rotation speeds ranging from 100 rpm to 800 rpm and applied loads from 2 kN to 20 kN under steady-state conditions. By careful control of the oil bath temperature, oil bearing temperature remained constant throughout at 65°C. During testing, the ultrasonic transducer mounted on Pin B was excited with a negative top-hat electrical pulse and the reflected time-domain signal was recorded. Pulse repetition frequency

was set to 80,000 times per second. Data is recorded over a five second period and a profile for each revolution is obtained. The average of these cycles is calculated per degree.

In Figures 14 and 15, film thickness profiles are compared against a predicted profile obtained via the Raimondi-Boyd model [18]. This method, formulated by solving the Reynolds Equation with numerical techniques, allows film thickness to be predicted by calculating the Sommerfeld number, S , a non-dimensional parameter defined as:

$$S = \left(\frac{r}{C}\right)^2 \frac{\mu LDN}{W} \quad (7)$$

Where r is the radius of the bearing and μ is lubricant dynamic viscosity.

Maximum and minimum boundaries for the Raimondi-Boyd prediction in the present study are due to uncertainty in bearing clearance. It can be observed that although clearance significantly affects predicted maximum film thickness, the effect on minimum film thickness appears to be negligible.

Near the point of minimum film thickness, predicted and experimental profiles are very consistent. However, differences are observed as the film gets thicker, particularly within the diverging region of the bearing. As shaft rotation passes 110° , both the amplitude and phase change model show an apparent sharp increase in measured film thickness. It is theorised that this is due to cavitation in the diverging region. Pressure reduces as the two surfaces separate, leading to the formation of air bubbles. The interface becomes what is effectively a steel-air boundary and as such there is near-total reflection of the acoustic wave [17].

In the bearing converging region, the ultrasonic models display slight variations in film thickness, for example in Figure 16 between 50° and 70° there is a clear dip in film thickness. It is thought that this decrease is due to elastic deformation of the bearing shells. Such deformations are a phenomenon not predicted by the Raimondi-Boyd model, which assumes the components are perfectly rigid [18].

As discussed previously, there is a limit to the measurement range of each method, dependent on the frequency of the transducer. There is not a simple cut-off film thickness, rather the sensitivity of each technique steadily decreases as film thickness increases. Limits are selected by drawing on previous experience, considering the signal quality of the reflected wave and the number of cycles averaged. Maximum reported film thickness has been restricted to $12.5 \mu\text{m}$ for the amplitude model, as this corresponds to a reflection coefficient of 0.99. Similarly, phase change has been restricted to $60 \mu\text{m}$, corresponding to a phase change of 0.025 rad.

Thick film measurements were obtained via the resonant dip technique. Results are within the Raimondi-Boyd prediction boundaries and follow the same curved profile. In Figure 14, the gap between minimum resonant dip value and maximum phase change value is small, at $5.6 \mu\text{m}$. Also, the methods follow similar profiles; this suggests good continuity between the two techniques.

Figure 16 displays tests performed at a range of rotation speeds, from 100 rpm to 800 rpm under a constant applied load of 10 kN, with results obtained via the phase change technique. As the shaft rotates more quickly, hydrodynamic pressure generated within the lubricant film increases, pushing the shaft and bearing surfaces apart with a greater force. This leads to a corresponding increase in the film thickness profile.

The top dead centre (TDC) position is also shown in Figure 16. By observing the position of minimum film thickness, attitude angle also increases with speed. Also note the small but sharp drop in film thickness at TDC; it is theorised this may be due to the thermocouple cable ejection channel in the bush behind the thin bearing shell located at TDC. It is possible that the bearing shell deformation is significant as the bearing shell area is unsupported. The position of this cable ejection channel is shown in Figure 17.

In Figure 18, the effect of applied load on film thickness profile may be observed. As one would expect, an increase in applied load leads to reduced film thickness across the whole profile, as well as a decrease in attitude angle when compared against the position of TDC. Again, as with Figure 16, a dip at TDC is observed. One may expect that if the cause is deformation then it would increase with higher load, however the opposite is observed. The reason may be that locally deforming the bearing to the same extent requires exponentially more energy as overall film thickness reduces and the interface stiffness is therefore greater. However, further investigation is required to understand this finding.

In Figure 19, the minimum film thickness calculated by both the amplitude and phase change techniques are compared against a Raimondi-Boyd prediction for all tests via the Sommerfeld number. Good agreement is seen between experimental results and theoretical prediction, with an average deviation from prediction of 9.6% (1.36 μm) and 4.1% (0.34 μm) for the phase change and amplitude techniques respectively. Each data point is obtained by taking an average of the minimum film thickness measurements for all cycles over the five second test. Error bars in this figure represent the variation in minimum film thickness measurement per cycle over this period to two standard deviations.

A difference between the phase and amplitude methods is introduced when sensor element temperature changes between the reference and measurement points. When rotation speed is high the time for heat transfer to occur is reduced between successive rotations, resulting in a more consistent pin temperature. As such, increasing rotation speed, and therefore increasing Sommerfeld number, leads to greater agreement between the two methods.

Minimum film thickness measurements obtained via the phase change technique are compared against conventional eddy current gap sensor measurements in Figure 20. Both techniques follow the same trends, however the phase change technique aligns with the Raimondi-Boyd prediction more closely, with an average deviation of 11.92% (0.92 μm) compared to 50.67% (4.31 μm) for gap sensor measurements at 200 rpm and 4.43% (0.76 μm) compared to 44.43% (5.05 μm) at 400 rpm. An apparent increase in film thickness at high loads is observed by the eddy current sensors, however as the probes are located away from the contact this error may be caused by deformation and thermal effects.

B. Misaligned Bearing Testing

To understand operation of the bearing platform under misaligned conditions, a series of tests were performed with variable shaft inclination relative to the bearing assembly. Misalignment was achieved by installing a rigid linkage to restrict the tilting motion of the bearing assembly. Then, the shaft was inclined by raising one support block incrementally by a set amount. In the previously discussed aligned bearing investigation, only the central pin, Pin B, was used. For misaligned testing three pins along the shaft's axial plane were used, these are Pins A, B and C; thus allowing a comparison of the film thickness profile in this plane. To ease comparison, the profile of Pin B has been shifted 90° to align with Pins A and C.

Figure 21 demonstrates that inducing misalignment has a significant effect on circumferential film thickness profiles. In this figure, a comparison between an aligned and misaligned case is shown. For the aligned case each film thickness profile is very similar, whereas for the misaligned case film thickness profiles vary substantially along the axis of the shaft.

Observing the change in circumferential film thickness profile measured by Pin C with variable shaft inclination angle, as shown in Figure 22, it can be seen that an increase in inclination leads to a reduction in film thickness across the entire circumference. However, as misalignment increases further, the film thickness reduction is not as substantial due to the non-linear relationship between pressure and film thickness, as demonstrated by both the Raimondi-Boyd prediction [18] and the Reynolds equation [20].

C. Shut-down Testing

This investigation studied the development of oil films during shut-down conditions. For shut-down testing, the bearing platform is set to a rotation speed of 200 rpm with a static load applied and allowed to reach steady-state conditions, with oil inlet temperature maintained at 40°C. A shut-down procedure is then initiated, in which the motor reduces rotation speed by a constant rate, 16 rpm/s, until stationary. Circumferential film thickness is measured throughout via Pin B. It should be noted that the flexible linkage was reinstalled for shut-down testing to ensure good bearing alignment.

Figure 23 and 24 show a non-linear reduction in minimum film thickness as shaft rotation speed decreases, with an applied static load of 6 kN and 10 kN respectively. Initially, circumferential film thickness profiles reduce only slightly, as observed by the the similarity between profiles at 200 rpm and 150 rpm in both Figures 23 and 24. However, this reduction becomes more rapid as the test progresses. Similarly, attitude angle decreases more rapidly as rotation speed reduces.

VII. DISCUSSION

The present work has demonstrated that the ultrasonic method is capable of high accuracy film thickness measurements under a range of operating conditions. Similar demonstrations have been made previously, however the key advance in this work has been the simultaneous application of the amplitude, phase change and resonant dip techniques in the circumferential measurement of oil films in journal bearings. This allows high accuracy measurements in the thin film region via the amplitude and phase change techniques, with more complete circumferential profiles obtained via the phase change technique, and thick film measurements via the resonant dip technique. Figure 25 highlights the regions around the bearing circumference in which

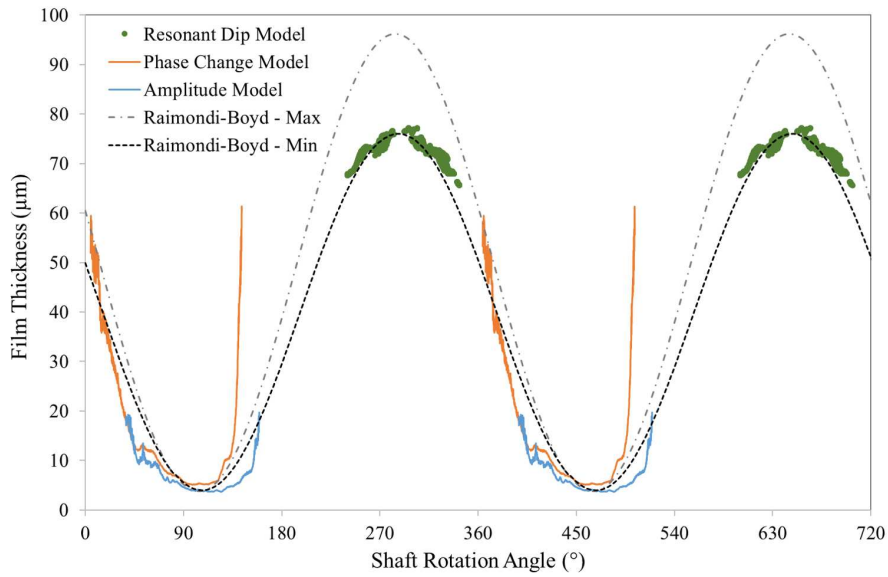


Fig. 14: Circumferential film thickness profile for 200 rpm, 20 kN test case.

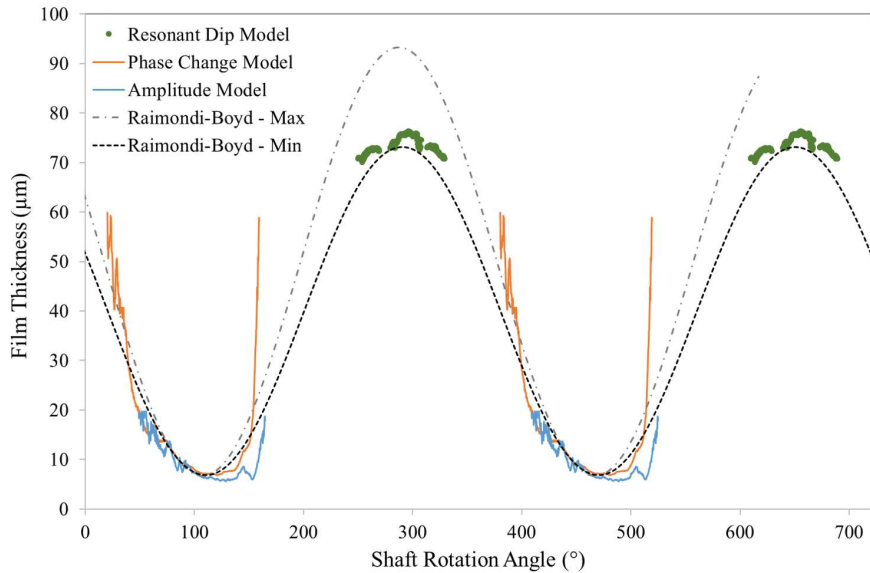


Fig. 15: Circumferential film thickness profile for 400 rpm, 20 kN test case.

each model may be applied.

Circumferential measurements allow the investigation of features which may have a dramatic effect on journal bearing performance, including deformation and cavitation. Understanding such phenomena has been achieved previously via numerical methods for rigid bearings with great success, however the problem becomes far more challenging when elastic effects must be considered, particularly for more advanced bearing designs. As such, an experimental technique which can analyse deformation and cavitation in more complex systems may be a useful tool in many applications.

In the current study, the ultrasonic technique consistently offered greater measurement accuracy than equivalent measurements obtained via eddy current gap sensors. This increased error arises due to the fundamental limitation of gap sensors in this configuration, offering only an indirect measurement outside the actual shaft-bearing interface. As such, the eddy current technique does not account for effects such as shaft bending and deformation in the bearing assembly. To enable a direct measurement, the gap sensors need to be located within the contact, which is both difficult to implement and would influence operation of the bearing system.

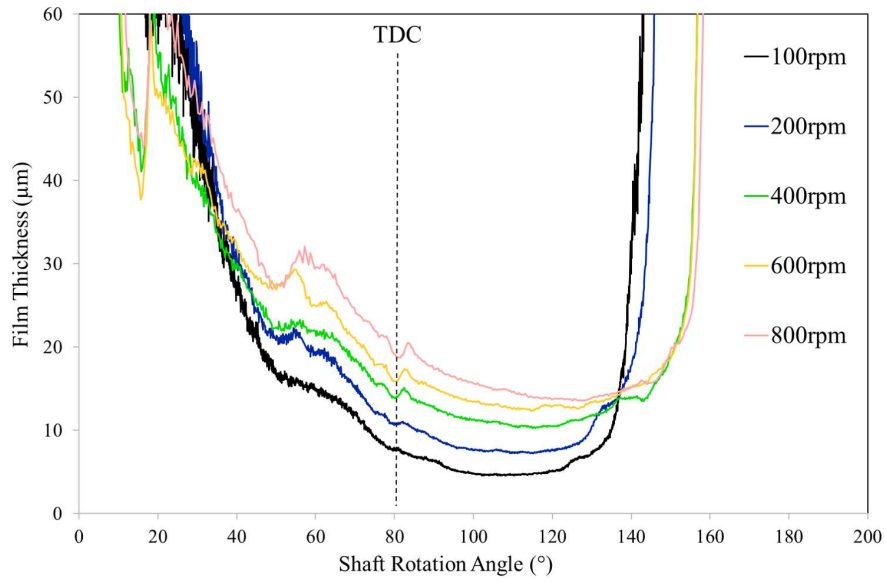


Fig. 16: Comparison of circumferential film thickness profiles for variable rotation speed, 10 kN constant applied load, obtained via the phase change technique.

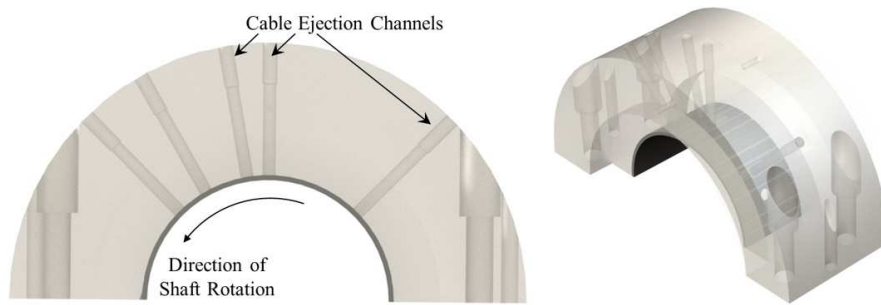


Fig. 17: Schematic of bearing bush, with cable ejection channels indicated

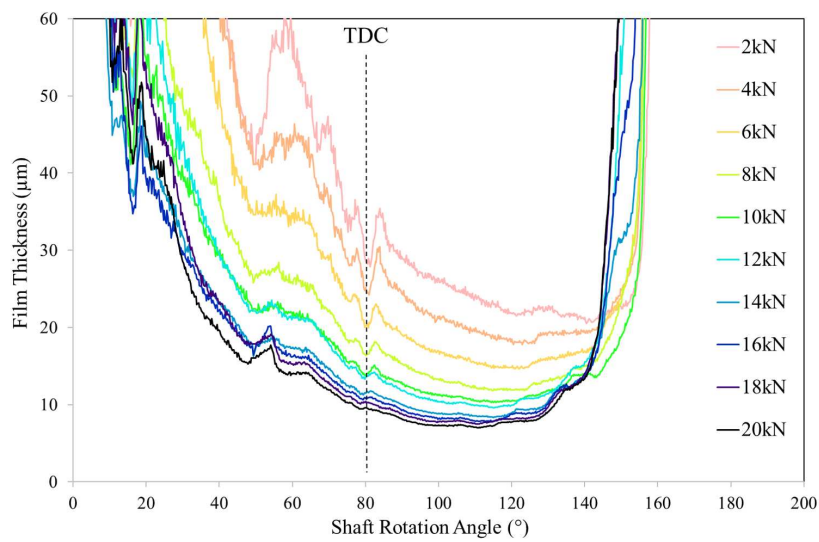


Fig. 18: Comparison of circumferential film thickness profiles for variable applied load, 400 rpm constant rotation speed, obtained via the phase change technique.

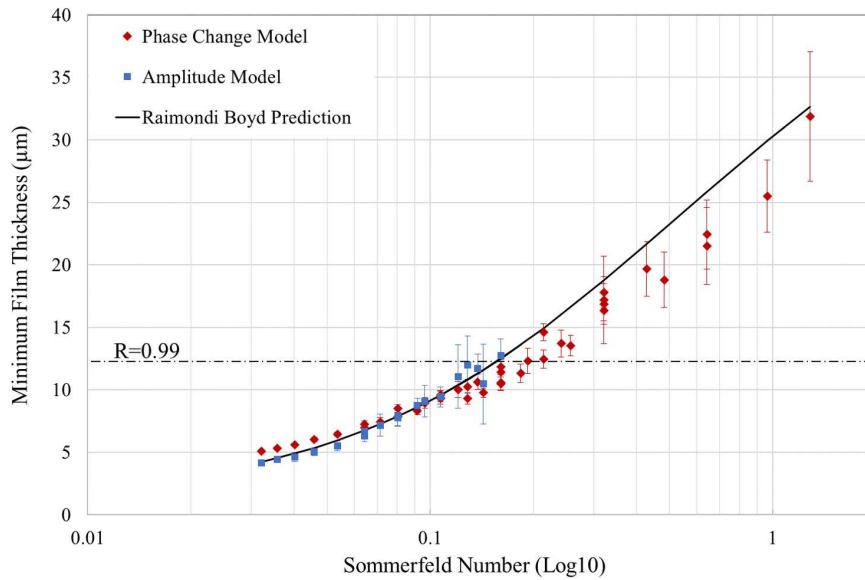


Fig. 19: Minimum film thickness measurements obtained via the amplitude and phase techniques compared against the Raimondi-Boyd theoretical model.

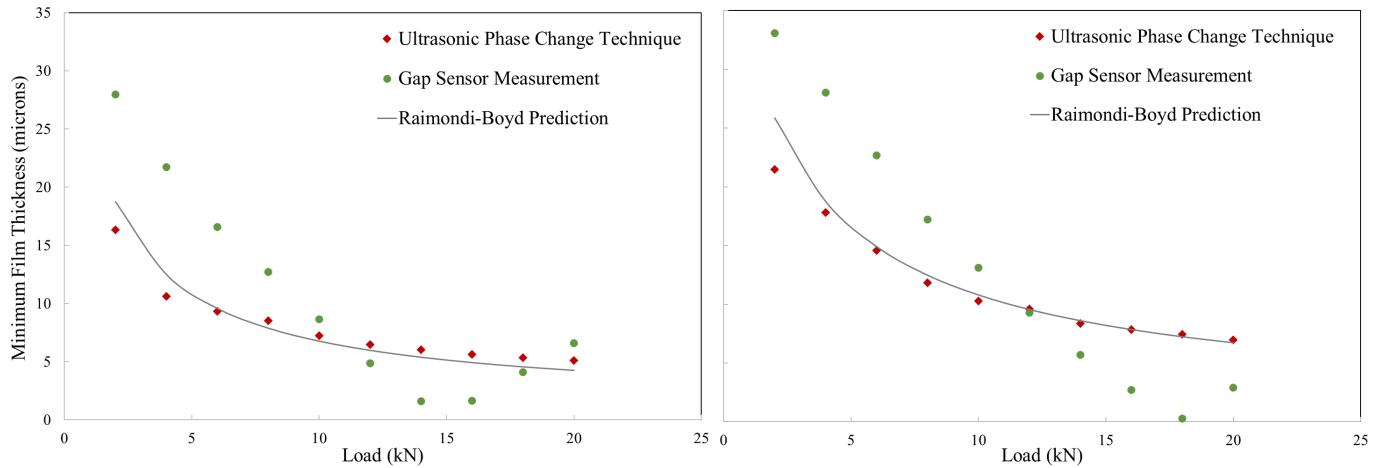


Fig. 20: Minimum film thickness against load for 200 rpm (left) and 400 rpm (right) rotation speeds, calculated by the phase change, gap sensor and Raimondi-Boyd techniques.

The smallest film measured in this investigation was $3.0 \mu\text{m}$. By applying the amplitude model in this system, lubricant films as low as $0.2 \mu\text{m}$ are easily measurable before changes in signal response are no longer clearly distinguishable from background noise. The bearing shells used in this investigation were measured to have a surface roughness of $0.7 \mu\text{m}$ and as such the system would be operating far within the boundary lubrication regime even before films approach $0.2 \mu\text{m}$. Additionally, almost all journal bearings operate with films much thicker than $0.2 \mu\text{m}$. For the phase change method minimum measurable film thickness is $0.7 \mu\text{m}$, which is suitable for the majority of journal bearing cases. However, if thinner film measurements were desired in an alternative application, such as in rolling element bearings, the implementation of higher frequency transducers would allow this capability.

In journal bearing testing the maximum measurable film thickness was $15 \mu\text{m}$ via the amplitude model and $60 \mu\text{m}$ via the phase change technique. If desired, increasing maximum measurable film thickness with these methods may be achieved with a lower frequency transducer element.

In this investigation the piezo-electric element is small (1 mm by 5 mm); the corresponding film thickness measurement

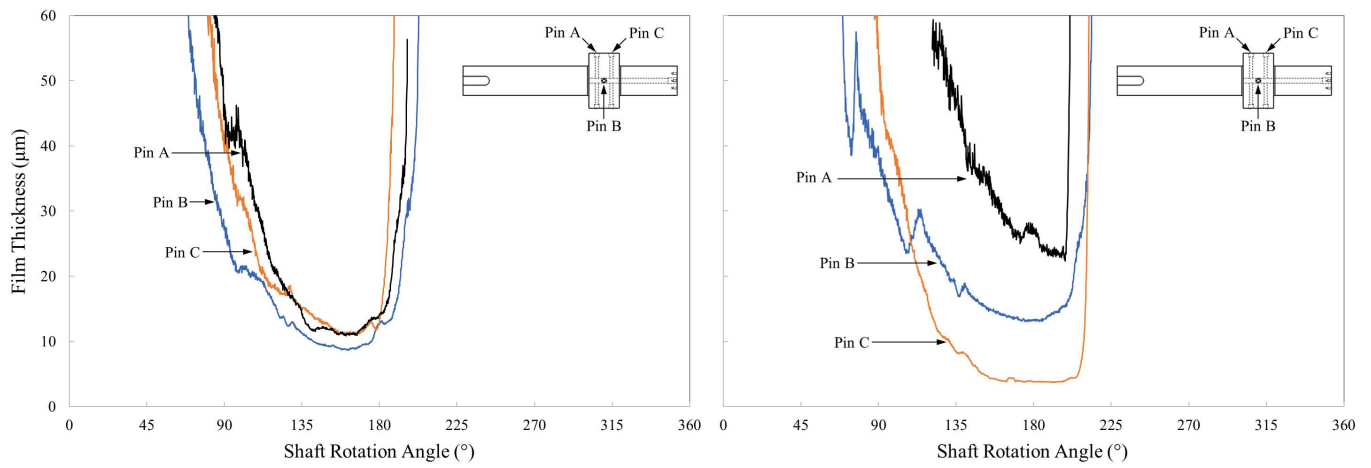


Fig. 21: Comparison of film thickness profiles along the shaft axis for an aligned (left) and misaligned (right) case, obtained via the phase change technique.

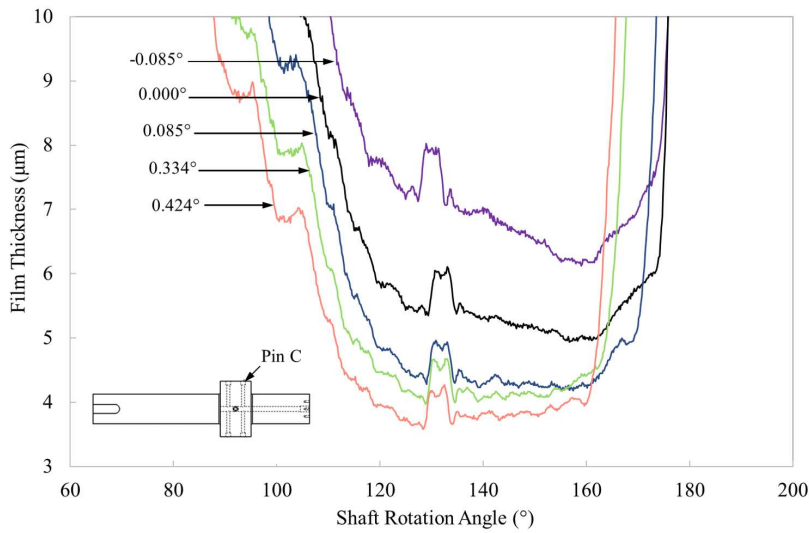


Fig. 22: Circumferential film thickness profile for Pin C for a range of misalignment angles, obtained via the phase change technique.

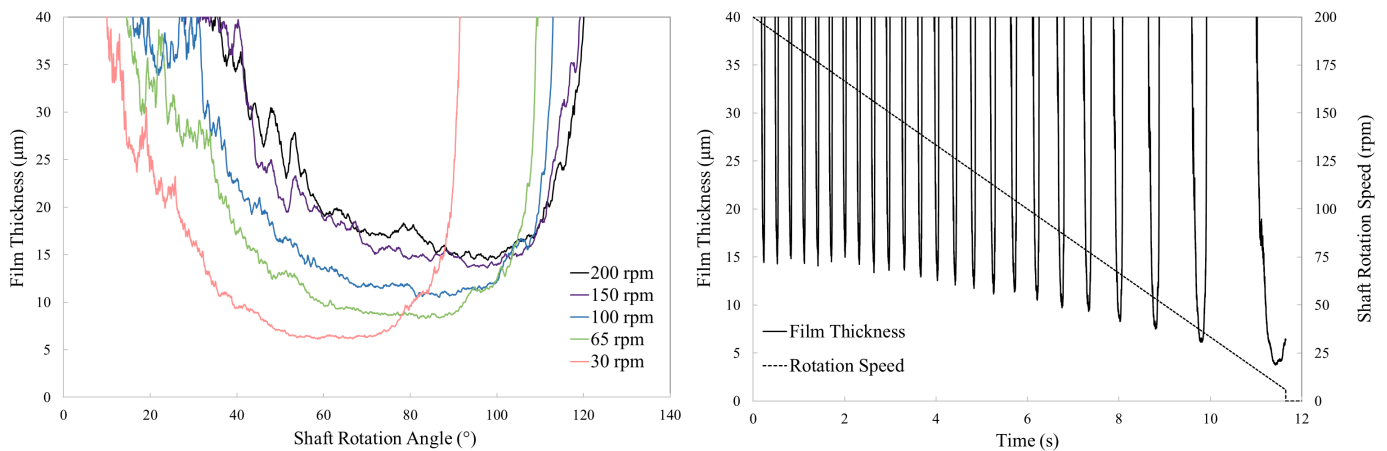


Fig. 23: Film thickness measurement during shut-down condition against rotation angle (left) and over time (right), 6 kN constant applied load, obtained via the phase change technique.

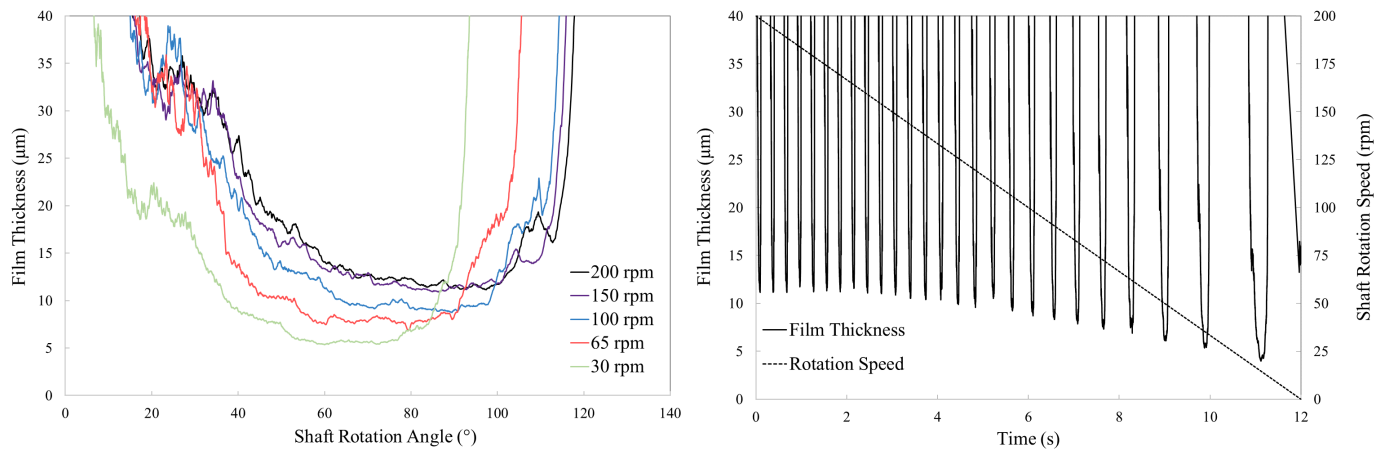


Fig. 24: Film thickness measurement during shut-down condition against rotation angle (left) and over time (right), 10 kN constant applied load, obtained via the phase change technique.

is approximately an average of film thicknesses over this area. This is certainly suitable for investigating features such as bulk deformation; however, making use of smaller elements would allow greater spatial resolution. Although, reducing the size of a piezo-electric element also decreases the magnitude of the generated wave and therefore signal amplitude due to the lower mass of the element. This would lead to a drop in signal-noise ratio and therefore accuracy in the film measurement.

The signal response from a reflected ultrasonic wave is often in the order of 10's mV, several orders of magnitude less than the initial wave generated. Therefore, any sources of electrical noise may have a significant detrimental effect on the accuracy and upper limit of the measurement technique. As such, there was concern using a slip ring to carry the electrical signal between the acquisition hardware and rotating shaft. However, effects were negligible and clear signal responses were obtained.

Prior to testing, the platform operated at moderate speeds and loads for an extended period to allow the system to run-in. This would ensure that the bearing and shaft surfaces remained consistent throughout testing. Additionally, bearing shell roughness was evaluated with a 3D profilometer before and after testing. Change in arithmetical mean roughness was negligible, remaining at $0.7 \mu\text{m}$.

In the present study an entire reflected signal is recorded in the time domain. This allows detailed analysis of the response but requires a large amount of disk space and an additional post-processing step. Live film thickness measurements could be obtained by recording only the FFT index amplitude and phase, rather than the complete time domain signal.

A single mineral oil was used throughout testing in the current study. However, the test platform has been designed so that changing lubricant types is a simple process. This extends the utility of the system as competing lubricant types may be compared, thus enabling the exploration of additional research topics. One such example is the study of EALs, as bearing failures have increased since their implementation and there is no consensus as to the cause.

A limitation of shut down testing in the current study is that the film thickness at very low rotation speeds, less than one full rotation before the shaft comes to rest, can not be measured accurately. This is a fundamental issue with film thickness sensors located in the shaft. Unless the sensor stops exactly at the point of minimum film thickness a near-zero rotation speed measurement cannot be obtained. Installing bearing mounted ultrasonic transducers around the minimum film region would overcome this shortcoming.

The installation of an in-line torque meter would enable further analysis into the relationship between film thickness and friction. As predicted by the Stribeck curve, during a shut-down procedure friction would initially decrease as viscous forces reduce, then sharply increase as the system transitions from the hydrodynamic lubrication regime into the mixed then boundary regimes. Performing such shut down tests on lubricants would offer an insight into their performance and range of suitable operation, particularly if compared against other oil types.

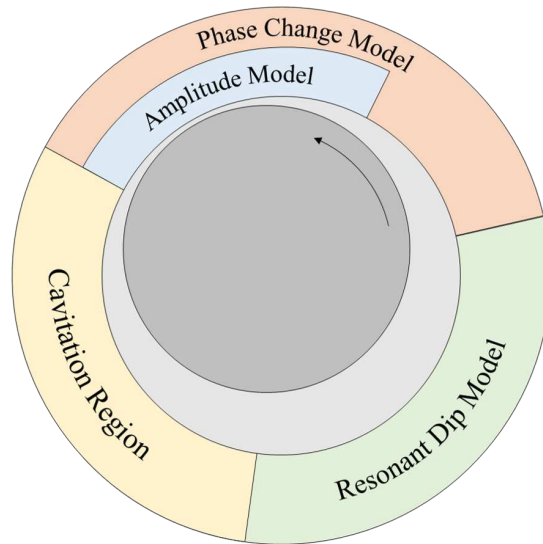


Fig. 25: Schematic of bearing, with measurement regions for each technique indicated.

VIII. CONCLUSION

This work has applied the amplitude, phase change and resonant dip ultrasonic techniques to obtain circumferential film thickness profiles in a journal bearing test platform under a range of aligned, misaligned and shut-down conditions. Results were compared against a Raimondi-Boyd prediction and conventional eddy current measurements. This study demonstrates that the amplitude model offers a high accuracy measurement for thin films, the phase change technique allows moderate film measurements and the resonant dip technique is capable of thick film measurements. Thus, the simultaneous application of all three methods enables high accuracy film thickness measurements around the circumference of a journal bearing using a single sensor.

Due to cavitation, quantitative film thickness measurements within the bearing diverging region are unobtainable via the ultrasonic methods applied in this study. However, this does provide an opportunity to investigate the onset of cavitation and its effects. Bearing deformation due to cable ejection channels was also observed; thus demonstrating that the ultrasonic technique is capable of detecting bearing deformation in a more general sense.

By restricting the tilting motion of the bearing assembly and using ultrasonic transducers along the axial plane of the shaft, circumferential film thickness profiles under varying degrees of shaft misalignment were obtained. Due to changing viscosity with pressure, the relation between set shaft inclination angle and resulting misalignment angle was shown to be non-linear.

Testing under shut-down conditions showed a reduction in film thickness as rotation speed decreased. The installation of a torque transducer and bearing mounted ultrasonic transducers would allow a comparison between film thickness and friction, with an expectation that the transition between hydrodynamic, mixed and boundary lubrication regimes may then be observed.

REFERENCES

- [1] T. M. Jalszynski and L. W. Evers, "Dynamic film measurements in journal bearings using an optical sensor," 1997.
- [2] F. X. Borrás, M. B. D. Rooij, and D. J. Schipper, "Rheological and wetting properties of environmentally acceptable lubricants (EALs) for application in stern tube seals," *Lubricants*, 2018.
- [3] A. Yano, E. Iwawaki, M. Mihara, and S. Yoshihara, "Study on the load carrying capacity of sliding bearing lubricated by synthetic ester oils," *Tribology Online*, vol. 10, no. 5, pp. 377–389, 2015.
- [4] G. Miranda, "The detection of journal bearing cavitation with use of ultrasound technology," Ph.D. dissertation, Case Western Reserve University, 2016.
- [5] S. B. Glavatskih, Uusitalo, and D. J. Spohn, "Simultaneous monitoring of oil film thickness and temperature in fluid film bearings," *Tribology International*, vol. 34, no. 12, pp. 853–857, 2001.

- [6] Q. Bai, F. Guo, P. L. Wong, and P. Jiang, "Online Measurement of Lubricating Film Thickness in Slider-on-Disc Contact Based on Dichromatic Optical Interferometry," *Tribology Letters*, vol. 65, no. 4, 2017.
- [7] R. S. Dwyer-Joyce, P. Harper, J. Pritchard, and B. W. Drinkwater, "Oil film measurement in polytetrafluoroethylene-faced thrust pad bearings for hydrogenerator applications," *Proceedings of the Institution of Mechanical Engineers, Part A: Journal of Power and Energy*, vol. 220, no. 6, pp. 619–628, 2006.
- [8] P. Harper, B. Hollingsworth, R. Dwyer-Joyce, and B. Drinkwater, "Journal bearing oil film measurement using ultrasonic reflection," in *Proceedings of the 29th Leeds-Lyon Symposium on Tribology*, vol. 41, 2003, pp. 469–476. [Online]. Available: <http://www.sciencedirect.com/science/article/pii/S016789220380161X>
- [9] D. Dowson, C. M. Taylor, C. I. N. Bearings, D. Dowson, and C. M. Taylor, "Cavitation in bearings," *Annual Review of Fluid Mechanics*, pp. 35–66, 1979. [Online]. Available: <http://www.annualreviews.org/doi/pdf/10.1146/annurev.fl.11.010179.000343>
- [10] A. Hernández-Peña, L. I. Farfan-Cabrera, and E. A. Gallardo-Hernández, "Investigation of the wear of engine journal bearings approaching severe lubrication conditions using a microabrasion tester," *Proceedings of the Institution of Mechanical Engineers, Part J: Journal of Engineering Tribology*, vol. 233, no. 12, pp. 1939–1949, 2019.
- [11] T. Reddyhoff, S. Kasolang, R. S. Dwyer-Joyce, and B. W. Drinkwater, "The phase shift of an ultrasonic pulse at an oil layer and determination of film thickness," *Proceedings of the Institution of Mechanical Engineers, Part J: Journal of Engineering Tribology*, vol. 219, no. 6, pp. 387–400, jun 2005. [Online]. Available: <http://journals.sagepub.com/doi/10.1243/135065005X34044>
- [12] R. Dwyer-Joyce, B. Drinkwater, and C. Donohoe, "The measurement of lubricant-film thickness using ultrasound," *Proceedings of the Royal Society Series A: Mathematical Physical and Engineering Sciences*, vol. 459, pp. 957–976, 2003. [Online]. Available: <http://eprints.whiterose.ac.uk/169/>
- [13] K. Zhang, P. Dou, T. Wu, and K. Feng, "An ultrasonic measurement method for full range of oil film thickness," *Engineering Tribology*, vol. 233, no. 3, pp. 481–489, 2019.
- [14] Z. Yu and A. J. Jaworski, "Impact of acoustic impedance and flow resistance on the power output capacity of the regenerators in travelling-wave thermoacoustic engines," *Energy Conversion and Management*, vol. 51, no. 2, pp. 350–359, 2010. [Online]. Available: <http://dx.doi.org/10.1016/j.enconman.2009.09.032>
- [15] A. Hunter, R. Dwyer-Joyce, and P. Harper, "Calibration and validation of ultrasonic reflection methods for thin-film measurement in tribology," *Measurement Science and Technology*, vol. 23, no. 10, p. 105605, oct 2012. [Online]. Available: <http://stacks.iop.org/0957-0233/23/i=10/a=105605?key=crossref.e4f4611f61f25dc0e7551d2cfc4ade1f>
- [16] A. Tverdokhlebov, "On the acoustoelastic effect," *The Journal of the Acoustical Society of America*, vol. 73, no. 6, pp. 2006–2012, 2005.
- [17] S. Kasolang, "Observations of Film Thickness Profile and Cavitation Around a Journal Bearing Circumference Observations of Film Thickness Profile and Cavitation Around a Journal Bearing Circumference," vol. 2004, 2008.
- [18] J. Raimondi, A. A. and Boyd, "A Solution for the Finite Journal Bearing and its Application to Analysis and Design," *ASLE Transactions*, vol. 1, no. 1, pp. 159–174, 1958.
- [19] C. Barus, "Isothermals, isopiestic and isometrics relative to viscosity," *American Journal of Science*, vol. 45, pp. 87–96, 1983.
- [20] D. Sfyris and A. Chasalevris, "An exact analytical solution of the Reynolds equation for the finite journal Bearing," *Tribology International*, no. May, 2012.